agronomy

Communication

Decision Support Tool to Predict Panicle Initiation in Aerobic Rice

Matthew Champness *, Carlos Ballester and John Hornbuckle

Centre for Regional and Rural Futures (CeRRF), Deakin University, Griffith, NSW 2680, Australia
* Correspondence: m.champness@deakin.edu.au

Abstract: Aerobic rice cultivation offers the potential to reduce irrigated water use. A multitude of challenges, such as cold sterility, drought stress, and labor shortages, limit its adoption in temperate rice-growing regions. Increasing the duration and extent of soil moisture tension between irrigation events has been demonstrated to slow crop development. Delaying panicle initiation (PI) beyond the optimal window can expose rice to cold nighttime temperatures during the cold sensitive early pollen microspore, severely reducing yield. Tools to assist Australian temperate farmers and researchers in the irrigation management of aerobic rice to ensure PI occurs during the optimal window do not yet exist. Using data collected from an aerobic rice experiment conducted in temperate Australia in 2020–2021 and 2021–2022, a predictive model was built to assist in forecasting PI based on the timing of irrigation. Estimation of the area on an hourly basis of the cumulative evapotranspiration with rainfall subtracted from pre-emergent irrigation to PI, defined as the irrigation deficit integral, was used to account for the frequency, duration, and extent of soil moisture deficit between irrigation events. The relationship between the irrigation deficit integral and the number of days from pre-emergent irrigation to PI (R^2 = 0.91) was used to build a model to predict PI with a root mean square error of 1.8 days for the validating data set. Furthermore, an example is provided of how the model can be used as a decision support tool to assist researchers and growers to schedule irrigation of aerobic rice to ensure PI occurs in a timely manner. This will increase the likelihood of high-yielding aerobic rice and may enhance the adoption of water-saving rice cultivation.

Keywords: decision support tool; water-saving irrigation; *Oryza sativa*; deficit irrigation; rice irrigation

Citation: Champness, M.; Ballester, C.; Hornbuckle, J. Decision Support Tool to Predict Panicle Initiation in Aerobic Rice. *Agronomy* **2023**, *13*, 789. https://doi.org/10.3390/agronomy13030789

Academic Editor: Jose Manuel Gonçalves

Received: 17 February 2023
Revised: 7 March 2023
Accepted: 7 March 2023
Published: 9 March 2023

1. Introduction

Research has shown a significant delay in rice phenological development under water-saving cultivation when compared with flooded rice systems [1–6]. Panicle initiation (PI) marks the end of vegetative growth and the beginning of the reproductive stage in rice development. Panicle initiation is an important crop development stage as it is the ideal time to sample and analyze plant nitrogen uptake and apply nitrogen in a relatively efficient manner as full crop canopy decreases volatilization risk [7]. Predicting PI can help assist growers in planning farm tasks and organizing contract fertilizer applicators.

The delay to reach PI and anthesis in water-saving rice has been demonstrated to increase with increasing moisture deficit [1–3,8]. Such delay can expose rice to unfavorable weather conditions during the cold sensitive early pollen microspore period and result in severe yield penalties [8]. In temperate Australia, the likelihood of cold-induced sterility can be reduced by ensuring PI occurs in the first 2 weeks of January [9]. Temperature has been found to be the primary environmental factor effecting crop development [10,11]; however, rice can also be photoperiod sensitive [12]. Thermal time has been used to model flooded rice crop development with common rice models; Oryza2000 [13] and CERES-Rice [14] have been adapted to different management and environmental conditions. As a result of the shoot apex being underwater for much of the season in flooded rice, incorporation of water temperature to model crop development has been found to enhance PI predictions in the USA [15]. However, in nonflooded conditions, this is not relevant, with models required for water-saving rice cultivation. While a PI predictor model has been developed for flooded and delayed permanent water rice cultivation in Australia [16], it is based on degree days. Therefore, such a model is majorly limited for adoption in aerobic rice as it does not account for the frequency, duration, or extent of moisture stress between irrigation events, which has a major effect on the time to reach PI [2,8]. Solar radiation also influences crop development [17] with prediction accuracy limited in models only accounting for thermal time.

The Australian rice industry has set an ambitious target to improve water productivity from 0.85 to 1.5 t/ML by 2026 [18,19] and identified the transition to aerobic cultivation as one option to achieve this ambitious target. However, commercial production of aerobic rice is not yet practiced in temperate Australia, with very few resources available to assist growers. This short communication aims to demonstrate a potential tool to enhance the ability of growers to predict PI dates and manage irrigation of aerobic rice to ensure PI is not delayed beyond optimal. Using data from a 2-year commercial aerobic rice trial in temperate Australia where various soil moisture deficits were investigated during the vegetative period, a model was built and verified using data from *c.v. Viand*, grown in heavy clay soils, to demonstrate the relationship between cumulative evapotranspiration between irrigation events and the number of days to reach PI. Examples are provided to demonstrate how this model could be used to create a decision support tool (DST). The aim of such DST is to assist fellow researchers and growers in making irrigation decisions that ensure panicle initiation is not delayed beyond the optimal window. This research will enhance growers' ability to maximize yield by reducing the risk of cold-induced sterility and may increase adoption of aerobic rice cultivation.

2. Materials and Methods

2.1. Model Creation and Validation

Crop data were used from a commercial aerobic rice experiment conducted in the temperate semiarid climate of the Murrumbidgee Valley in southeastern Australia near Griffith, NSW (34°17′18″ S, 146°03′03″ E), during the 2020–2021 and 2021–2022 season as detailed in [8]. In brief, various irrigation thresholds were investigated using watermark sensors (Model 200SS, Irrometer Company Inc., Riverside, CA, USA) installed to a depth of 15 cm and connected to loggers that sent data regularly to the cloud. The irrigation thresholds were applied during the vegetative period from establishment until PI in a rice crop grown across 9 bays, providing a total of 18 replicate data sets for analysis. The soil was a typical rice-growing soil for the region, classified as a self-mulching clay with a brown A horizon of 30 cm over a dense red B horizon [20]. This temperate region relies on gravity surface irrigation for rice production as summers are typically hot, with low humidity and an average in-season rainfall of 150 mm and an evapotranspiration of 1150 mm [21]. *C.v. Viand* was drill sown at a rate of 130 and 120 kg/ha in years 1 and 2, respectively, and is a short-season semidwarf variety (106 days sowing to anthesis [22,23]).

Nitrogen (N) was applied as granular urea (46% N) at a rate of 220 kg N/ha as a three-way split. This rate was determined based on high-yielding rice (>10 t/ha) N requirements for a heavy clay soil in the Murrumbidgee region, with consideration for higher N losses than normal due to aerobic growing conditions. As detailed in [8], in-season (15 October–30 April) rainfall totaled 175 and 352 mm with a reference evapotranspiration of 1259 and 1100 mm for years 1 and 2, respectively. Yields ranged from 3.6 to 8.1 t/ha with 7.95 and 4.65 ML/ha irrigation water applied in Year 1 and 2, respectively. Total water productivity ranged from 0.37 to 0.93 t/ML, and irrigated water productivity 0.43 to 1.62 t/ML, depending on the irrigation regime and year calculated as per [24]. PI was declared when the panicle could be identified with the naked eye in three out of 10 tillers [7]. Extending soil moisture deficit from −15 to −40 kPa was found to delay PI by an average of 14 days, with an irrigation threshold of −70 kPa further delaying PI. The data were combined with hourly reference evapotranspiration (ETo) as calculated from nearby weather observations using the standardized ASCE equation [25] to estimate cumulative reference evapotranspiration between irrigation events up until PI.

To account for the extent, duration, and frequency of soil moisture deficit from pre-emergent irrigation until PI, the irrigation deficit integral (IDI) for this period was calculated. The IDI is the summation of the areas formed by the cumulative evapotranspiration between two time intervals at what time ETo (mm) was calculated (the area of a right-angled trapezoid) between irrigation events (cumulative ETo resets to zero when there is an irrigation event). Hourly ETo data were used to create the model, with the IDI (mm * hour) calculated from pre-emergent irrigation (t = 0) to PI (t = n) according to the following equation:

$$\sum_{t=0}^{t=n} \frac{\left(ETcum_{tj} + ETcum_{tj+1}\right)}{2} \times \left(t_{j+1} - t_j\right) \quad (1)$$

where $ETcum_{tj}$ is cumulative ETo with rainfall subtracted at time j, when an ETo measure was taken, and $ETcum_{tj+1}$ is the time of the subsequent ETo measure. An example of a time interval is shown in Figure 1.

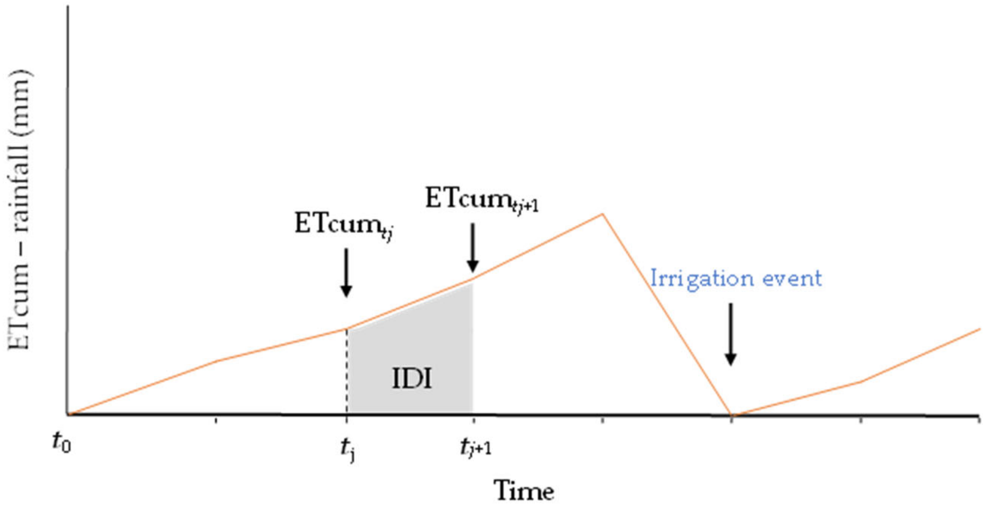

Figure 1. Representation of how the irrigation deficit integral (IDI) was calculated for each time interval as per Equation (1). The first and last periods between irrigation events are triangles; however, the trapezoid area was still used in these instances as one side equaled zero.

A random sample of 13 data sets was used to build the linear model, with five random data sets used for model evaluation. The IDI was found to be correlated to the number of days from pre-emergent irrigation to PI. This enabled a predictive model to be built, with the root mean square error (RMSE) calculated between the predicted number of days to PI and the actual number of days to PI. The model was then substantiated using the validating data with performance assessed using RMSE.

2.2. Demonstration as a Decision Support Tool

Combining in-season data and long-term average ETo data or forecast ETo, the model presented provides foundations for a DST to predict whether PI will occur by the desired date based on a predetermined irrigation schedule. An example of how the model could be used as a DST was demonstrated using 10-year average daily ETo data at Griffith, NSW, Australia (BOM 2022) for two aerobic rice fields under different irrigation regimes. Input data included pre-emergent irrigation date, desired PI date, and ETo irrigation threshold. Using the number of days from pre-emergent irrigation until the desired PI date, the model was used to calculate the maximum permissible irrigation deficit integral to ensure timely PI. In this case, IDI was calculated daily (historical ETo data were available on a daily basis), with the area resulting from a day without an irrigation event being added to the previous areas and cumulative ETo resetting to zero when an irrigation event or significant rainfall occurred. In this case, the area was still calculated as per Figure 1, with the time interval being daily. In instances where the model predicts that PI cannot be achieved by the desired date, the DST can recommend to the user for the irrigation threshold to be reduced. The model was built using short-season semidwarf *c.v. Viand* grown in heavy clay soils, and accuracy may be limited in other soil types with different cultivars or seasons.

3. Results and Discussion

3.1. Model Creation and Validation

Daily ETo and rainfall data from year 1 are provided in Figure 2A. An example of cumulative ETo with rainfall subtracted from pre-emergent irrigation until PI is provided in Figure 2B for three individual replicates sown on the same day with different irrigation regimes. The date when PI occurred for the individual replicates is indicated by dots. Cumulative ETo was reset to 0 mm at the time of irrigation or significant rainfall. The PI dates and irrigation deficit integral calculated as per Equation (1) for the three replicates are presented in Table 1 with different colors used to represent the three individual replicates.

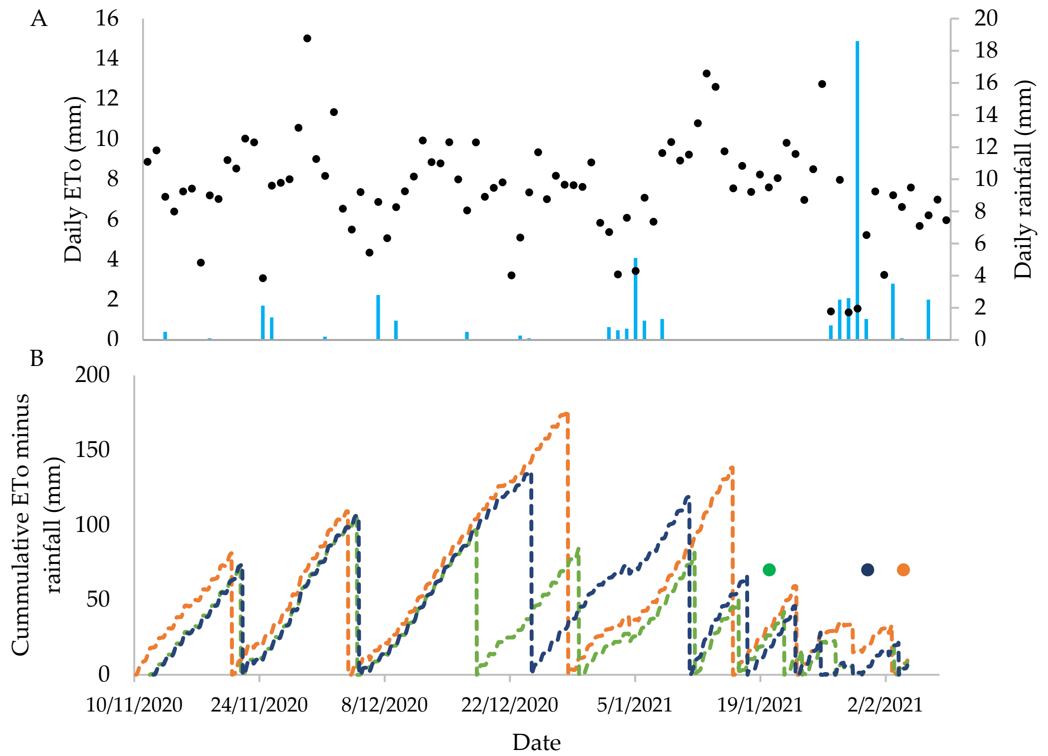

Figure 2. (**A**) Daily ETo (mm) shown as black dots and rainfall (mm) as blue bars from pre-emergent irrigation until PI. (**B**) Cumulative ETo with rainfall subtracted (mm) between irrigation events for three individual replicates (−15 kPa—green, −40 kPa—blue, −70 kPa—orange) from pre-emergent irrigation until panicle initiation, which is illustrated by dots. Note that the green and blue lines show similar cumulative ETo during the first three deficit events. The deficit integral of each replicate was calculated as per Equation (1).

Table 1. Panicle initiation date and irrigation deficit integral (IDI) of corresponding replicates presented in Figure 2.

Replicate	PI Date	IDI
−15 kPa (green)	20 January 2022	2690
−40 kPa (blue)	31 January 2021	3739
−70 kPa (orange)	4 February 2021	4266

The irrigation deficit integral of the parameterizing data was strongly correlated to the number of days from pre-emergent irrigation to PI (R^2 = 0.91, Figure 3A). The linear relationship was used to predict the number of days until PI in the validating data using the following equation:

$$\text{Number of days from pre-emergent irrigation to PI} = 0.0104 \times \text{IDI} + 41.439 \quad (2)$$

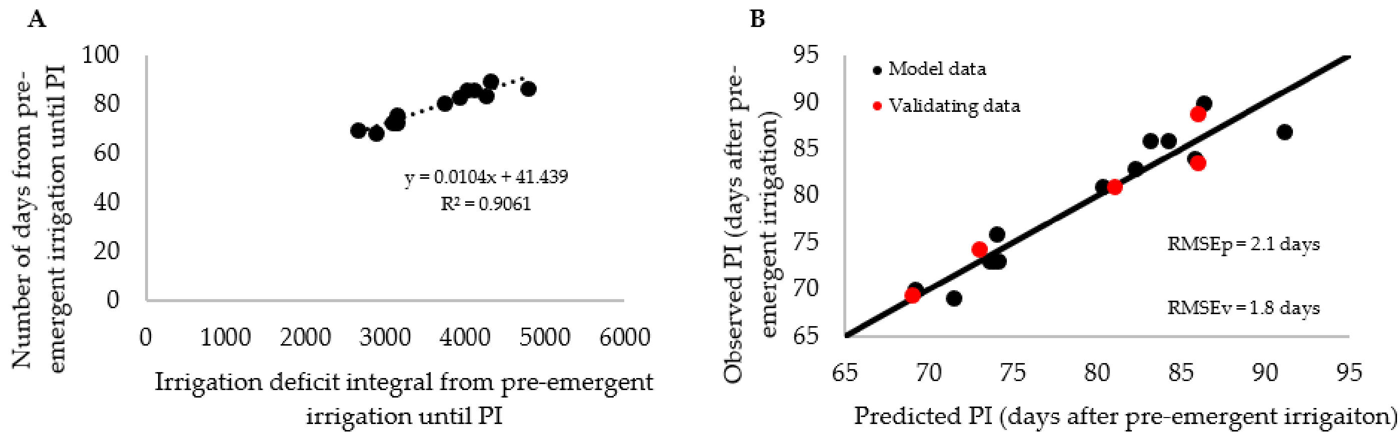

Figure 3. (**A**) Irrigation deficit integral from pre-emergent irrigation until PI versus the number of days from pre-emergent irrigation until PI (n = 13). (**B**) Modelled versus predicted number of days to PI with black dots representing parameterizing data and red dots the validating data. The RMSE of the parameterizing data (RMSEp) totaled 2.1 days and the validating data (RMSEv) 1.8 days.

The modelled data recorded a parameterizing RMSE of 2.1 days, and the validating data achieved an RMSE of 1.8 days. The modelled and observed number of days to reach PI is plotted in Figure 3B to illustrate the model fit.

3.2. Demonstration of the Model as a Decision Support Tool

Soil moisture tension was used to initiate irrigation in the data used to create the model; however, farmers and researchers alike may choose to schedule irrigation based on cumulative evapotranspiration thresholds as conducted by [6].

Required input parameters for the model to be used as a DST are colored gray in Table 2. It must be noted that the irrigation threshold chosen by the user is not applied to the second or third irrigation events as these are determined by agronomic reasons (e.g., plant emergence and herbicide application). These generally occur 10 days after the previous irrigation and, therefore, were used for this example.

Based on the user-entered dates, calculation of the number of days from pre-emergent irrigation to PI can be performed, and the maximal irrigation deficit integral calculated using the model. Using long-term average ETo (mm) and resetting cumulative ETo at the time of an irrigation event, the forecast irrigation deficit integral can be calculated (Table 3). It can be seen in Table 2 that the cumulative irrigation deficit was forecast to be 3680 and 4370 on 7 January for Fields A and B, respectively. However, the model calculated a maximal irrigation deficit integral of 4036 to achieve target PI on time (Table 3). Therefore, it is forecast that only Field A will achieve PI on time, and a reduced irrigation threshold or earlier per-emergent irrigation should occur in Field B for PI to occur within the desired window (Table 3). To improve accuracy during the season, integration of actual in-season ETo could be incorporated, with forecast ETo used to assist in shorter-term irrigation scheduling.

Table 2. Demonstration of the model used as a decision support to test whether PI is predicted to occur before the desired date based on input parameters from Table 2. The colored background is used to highlight when an irrigation event was scheduled as a result of surpassing the respective ETo threshold.

		Field A: ETo Threshold = 100			Field B: ETo Threshold = 120		
Date	**Long-Term Daily Av ETo**	**Cumulative ET_o (mm)**	**Daily Irrigation Deficit Integral**	**Cumulative Irrigation Deficit Integral**	**Cumulative ETo (mm)**	**Daily Irrigation Deficit Integral**	**Cumulative Irrigation Deficit Integral**
15/10/2022	6.2	0.0	0.0	0	0.0	0.0	0
16/10/2022	6.3	6.3	3.1	3	6.3	3.1	3
17/10/2022	5.0	11.2	8.7	12	11.2	8.7	12
18/10/2022	5.6	16.9	14.0	26	16.9	14.0	26
19/10/2022	5.8	22.6	19.7	46	22.6	19.7	46
20/10/2022	6.0	28.6	25.6	71	28.6	25.6	71
21/10/2022	6.1	34.7	31.7	103	34.7	31.7	103
22/10/2022	6.2	40.9	37.8	141	40.9	37.8	141
23/10/2022	6.0	46.9	43.9	185	46.9	43.9	185
24/10/2022	5.7	52.6	49.8	234	52.6	49.8	234
25/10/2022	6.6	0.0	26.3	261	0.0	26.3	261
26/10/2022	5.7	5.7	2.9	264	5.7	2.9	264
27/10/2022	6.1	11.9	8.8	272	11.9	8.8	272
28/10/2022	6.1	18.0	14.9	287	18.0	14.9	287
29/10/2022	6.2	24.2	21.1	308	24.2	21.1	308
30/10/2022	6.2	30.3	27.2	336	30.3	27.2	336
31/10/2022	6.0	36.4	33.3	369	36.4	33.3	369
1/11/2022	6.9	43.3	39.8	409	43.3	39.8	409
2/11/2022	6.9	50.2	46.8	456	50.2	46.8	456
3/11/2022	5.5	55.7	53.0	508	55.7	53.0	508
4/11/2022	6.4	0.0	27.9	536	0.0	27.9	536
5/11/2022	6.2	6.2	3.1	539	6.2	3.1	539
6/11/2022	6.5	12.7	9.5	549	12.7	9.5	549
7/11/2022	5.9	18.6	15.7	565	18.6	15.7	565
8/11/2022	6.5	25.1	21.9	586	25.1	21.9	586
9/11/2022	6.6	31.8	28.4	615	31.8	28.4	615
10/11/2022	7.2	38.9	35.3	650	38.9	35.3	650
11/11/2022	6.8	45.7	42.3	693	45.7	42.3	693
12/11/2022	6.9	52.7	49.2	742	52.7	49.2	742
13/11/2022	6.0	58.7	55.7	798	58.7	55.7	798
14/11/2022	6.7	65.3	62.0	860	65.3	62.0	860
15/11/2022	6.5	71.9	68.6	928	71.9	68.6	928
16/11/2022	5.9	77.8	74.8	1003	77.8	74.8	1003
17/11/2022	7.0	84.8	81.3	1084	84.8	81.3	1084
18/11/2022	7.7	92.5	88.7	1173	92.5	88.7	1173
19/11/2022	8.2	100.7	96.6	1269	100.7	96.6	1269
20/11/2022	8.9	0.0	50.3	1320	109.5	105.1	1375
21/11/2022	9.4	9.4	4.7	1324	118.9	114.2	1489
22/11/2022	7.9	17.2	13.3	1338	126.8	122.8	1612
23/11/2022	6.8	24.1	20.7	1358	0.0	63.4	1675
24/11/2022	6.7	30.8	27.4	1386	6.7	3.3	1678
25/11/2022	7.3	38.1	34.4	1420	14.0	10.4	1689
26/11/2022	6.8	44.9	41.5	1462	20.8	17.4	1706
27/11/2022	7.4	52.3	48.6	1510	28.2	24.5	1731
28/11/2022	8.3	60.6	56.5	1567	36.5	32.4	1763
29/11/2022	7.8	68.4	64.5	1631	44.3	40.4	1803
30/11/2022	8.3	76.7	72.5	1704	52.6	48.5	1852
1/12/2022	7.6	84.2	80.5	1784	60.2	56.4	1908
2/12/2022	7.3	91.5	87.9	1872	67.4	63.8	1972
3/12/2022	7.3	98.8	95.2	1967	74.8	71.1	2043
4/12/2022	7.5	106.3	102.6	2070	82.2	78.5	2122
5/12/2022	7.3	0.0	53.1	2123	89.5	85.9	2208

Table 2. *Cont.*

		Field A: ETo Threshold = 100			Field B: ETo Threshold = 120		
Date	Long-Term Daily Av ETo	Cumulative ET_o (mm)	Daily Irrigation Deficit Integral	Cumulative Irrigation Deficit Integral	Cumulative ETo (mm)	Daily Irrigation Deficit Integral	Cumulative Irrigation Deficit Integral
6/12/2022	7.3	7.3	3.6	2127	96.8	93.1	2301
7/12/2022	7.8	15.0	11.1	2138	104.5	100.6	2401
8/12/2022	7.5	22.5	18.8	2157	112.0	108.3	2510
9/12/2022	7.7	30.3	26.4	2183	119.8	115.9	2625
10/12/2022	8.1	38.3	34.3	2217	127.8	123.8	2749
11/12/2022	8.3	46.6	42.4	2260	0.0	63.9	2813
12/12/2022	8.2	54.8	50.7	2310	8.2	4.1	2817
13/12/2022	8.5	63.3	59.0	2369	16.7	12.5	2830
14/12/2022	7.9	71.1	67.2	2437	24.6	20.6	2850
15/12/2022	7.3	78.5	74.8	2512	31.9	28.2	2879
16/12/2022	8.2	86.7	82.6	2594	40.1	36.0	2915
17/12/2022	8.6	95.3	91.0	2685	48.7	44.4	2959
18/12/2022	9.8	105.1	100.2	2785	58.5	53.6	3013
19/12/2022	9.5	0.0	52.5	2838	68.0	63.2	3076
20/12/2022	9.3	9.3	4.7	2842	77.3	72.6	3148
21/12/2022	8.2	17.5	13.4	2856	85.5	81.4	3230
22/12/2022	8.6	26.1	21.8	2878	94.0	89.7	3320
23/12/2022	8.3	34.4	30.2	2908	102.3	98.2	3418
24/12/2022	9.0	43.4	38.9	2947	111.3	106.8	3525
25/12/2022	8.3	51.6	47.5	2994	119.6	115.5	3640
26/12/2022	8.7	60.3	56.0	3050	128.3	124.0	3764
27/12/2022	9.4	69.8	65.1	3115	0.0	64.2	3828
28/12/2022	10.0	79.8	74.8	3190	10.0	5.0	3833
29/12/2022	9.2	89.0	84.4	3275	19.2	14.6	3848
30/12/2022	8.8	97.7	93.3	3368	28.0	23.6	3871
31/12/2022	8.5	106.2	102.0	3470	36.4	32.2	3904
1/01/2023	8.4	0.0	53.1	3523	44.9	40.6	3944
2/01/2023	8.8	8.8	4.4	3527	53.6	49.2	3993
3/01/2023	9.0	17.8	13.3	3541	62.6	58.1	4052
4/01/2023	8.9	26.7	22.2	3563	71.5	67.1	4119
5/01/2023	8.0	34.7	30.7	3593	79.5	75.5	4194
6/01/2023	8.3	42.9	38.8	3632	87.8	83.7	4278
7/01/2023	9.1	52.0	47.5	3680	96.9	92.3	4370

Table 3. Input data required from growers (grey) for the decision support tool with positive outcomes displayed in green and negative outcomes in red.

Field	ETo Irrigation Threshold (mm)	Pre-Emergent Irrigation Date	Target PI Date	Number of Days to Target PI	Modelled Max Irrigation Deficit Integral to Achieve Target PI	Forecast Irrigation Deficit Integral by Target PI	Outcome
A	100	15/10/2022	7/1/2023	84	4036	3680	PI should occur by the desired date
B	120	15/10/2022	7/1/2023	84	4036	4370	Consider reducing the irrigation threshold or earlier pre-emergent irrigation

4. Conclusions

This communication demonstrates a relationship between the summation of the areas formed by the cumulative evapotranspiration between irrigation events, here called irrigation deficit integral, and the number of days required to achieve PI in aerobic rice systems. The model built from two seasons of data using *c.v. Viand* in a heavy clay soil was able to predict the number of days to PI within 1.8 days using the irrigation deficit integral.

Aerobic rice cultivation may provide a significant opportunity for the Australian rice industry to improve water productivity; however, growers require assistance as they transition from permanently flooded rice. The model presented can be used as a decision support tool for future researchers and growers as a starting point to make irrigation decisions aimed at ensuring PI is achieved within the desired window. However, accuracy may be limited with different cultivar selection or soil types. Nevertheless, it offers the potential to maximize the likelihood of a successful rice yield and may enhance the adoption of aerobic rice cultivation. As research and adoption of aerobic rice culture continues in temperate Australia, more data can be included to test and refine the model across seasons, cultivars, and soil types.

Author Contributions: Conceptualization, M.C.; methodology, M.C., C.B. and J.H.; formal analysis, M.C.; investigation, M.C.; writing—original draft preparation, M.C.; writing—review and editing, J.H. and C.B.; funding acquisition, J.H. All authors have read and agreed to the published version of the manuscript.

Funding: This project received funding from the Australian government's Future Drought Fund.

Institutional Review Board Statement: Not applicable.

Informed Consent Statement: Not applicable.

Data Availability Statement: The data presented in this study are available on request from the corresponding author.

Acknowledgments: The authors acknowledge Darrell Fiddler and DeBortoli Wines for providing the trial site and for their assistance throughout the study.

Conflicts of Interest: The authors declare no conflict of interest.

References

1. Blackwell, J.; Meyer, W.S.; Smith, R.C.G. Growth and Yield of Rice Under Sprinkler Irrigation on A Free-Draining Soil. *Aust. J. Exp. Agric.* **1985**, *25*, 636–641. [CrossRef]
2. Heenan, D.P.; Thompson, J.A. Growth, Grain Yield and Water Use of Rice Grown Under Restricted Water Supply in New South Wales. *Aust. J. Exp. Agric.* **1984**, *24*, 104–109. [CrossRef]
3. Muirhead, W.A.; Blackwell, J.; Humphreys, E.; White, R.J.G. The Growth and Nitrogen Economy of Rice under Sprinkler and Flood Irrigation in South East Australia-I. Crop Response and N Uptake. *Irrig. Sci.* **1989**, *10*, 183–199. [CrossRef]
4. Dunn, B.; Aerobic Rice Delay in Development, Yanco, Australia. Personal communication, 2022.
5. Wood, R.; Dunn, B.; Waters, D.L.E.; Blanchard, C.L.; Mawson, A.J.; Oli, P. Effect of Agronomic Management on Rice Grain Quality Part III: Australian Water-Saving Irrigation Practices. *Cereal Chem.* **2020**, *98*, 249–262. [CrossRef]
6. Dunn, B.; Gaydon, D. Rice Growth, Yield and Water Productivity Responses to Irrigation Scheduling Prior to the Delayed Application of Continuous Flooding in South-East Australia. *Agric. Water Manag.* **2011**, *98*, 1799–1807. [CrossRef]
7. Dunn, T.; Dunn, B. Identifying Panicle Initiation in Rice. *Primefact New South Wales Dep. Prim. Ind.* **2018**, *1278*, 1–4.
8. Champness, M.; Ballester, C.; Hornbuckle, J. Effect of Soil Moisture Deficit on Aerobic Rice in Temperate Australia. *Agronomy* **2023**, *13*, 168. [CrossRef]
9. NSW DPI. *Rice Growing Guide*, 2nd ed.; Ward, R., Ed.; NSW Department of Primary Industries: Yanco, Australia, 2021.
10. Gao, D.; Jln, Z.; Huang, Y.; Zhang, D. Rice Clock Model a Computer Model to Simulate Rice Development. *Agric. For. Meteorol.* **1992**, *60*, 1–16. [CrossRef]
11. XinYou, Y.; Kropff, M.J.; Goudriann, J. Differential Effects of Day and Night Temperature on Development to Flowering in Rice. *Ann. Bot.* **1996**, *77*, 203–213.
12. Yin, X.; Kropff, M.J.; Horie, T.; Nakagawa, H.; Centeno, H.G.S.; Zhu, D.; Goudriaan, J. A Model for Photothermal Responses of Flowering in Rice. I. Model Description and Parameterization. *Field Crops Res.* **1997**, *51*, 189–200. [CrossRef]
13. Bouman, B.A.M. Description and Evaluation of the Rice Growth Model ORYZA2000 under Nitrogen-Limited Conditions. *Agric. Syst.* **2006**, *87*, 249–273. [CrossRef]
14. Alocilja, E.C.; Ritchie, J.T. A Model for the Phenology of Rice. In *Predicting Crop Phenology*; Hodges, T., Ed.; CRC Press: Boca Raton, FL, USA, 1991; pp. 181–189.
15. Sharifi, H.; Hijmans, R.J.; Hill, J.E.; Linquist, B.A. Water and Air Temperature Impacts on Rice (Oryza Sativa) Phenology. *Paddy Water Environ.* **2018**, *16*, 467–476. [CrossRef]
16. Darbyshire, R.; Crean, E.; Dunn, T.; Dunn, B. Predicting Panicle Initiation Timing in Rice Grown Using Water Efficient Systems. *Field. Crops Res.* **2019**, *239*, 159–164. [CrossRef]

17. Li, S.; Fleisher, D.; Timlin, D.; Reddy, V.R.; Wang, Z.; McClung, A. Evaluation of Different Crop Models for Simulating Rice Development and Yield in the U.S. Mississippi Delta. *Agronomy* **2020**, *10*, 1905. [CrossRef]
18. Agrifutures Australia. *AgriFutures Rice Program Strategic RD&E Plan (2021–2026)*; Agrifutures Australia: Wagga Wagga, NSW, Australia, 2021; Available online: https://agrifutures.com.au/wp-content/uploads/2022/11/rice-RDE-.pdf (accessed on 10 October 2022).
19. Groat, M. *The Future of Australian Rice Production: A Focus on Water Use Efficiency in the Australian Temperate Rice System*; No. Project 1704; Nuffield Australia: Sydney, Australia, 2020; pp. 1–44.
20. Hornbuckle, J.; Christen, E. Physical Properties of Soils in the Murrumbidgee and Coleambally Irrigation Areas. *CSIRO L. Water Tech. Rep.* **1999**, *17*, 175.
21. Humphreys, E.; Lewin, L.G.; Khan, S.; Beecher, H.G.; Lacy, J.M.; Thompson, J.A.; Batten, G.D.; Brown, A.; Russell, C.A.; Christen, E.W.; et al. Integration of Approaches to Increasing Water Use Efficiency in Rice-Based Systems in Southeast Australia. *Field. Crops Res.* **2006**, *97*, 19–33. [CrossRef]
22. Reinke, R.; Snell, P. *Rice Improvement II—Developing New Varieties for the Australian Rice Industry*; Rural Industries Research and Development Corporation: Canberra, Australia, 2009.
23. NSW DPI. *Rice Variety Guide 2020–2021*; Troldahl, D., Ed.; NSW Department of Primary Industries: Yanco, Australia, 2021.
24. Tuong, T.P.; Bouman, B.A.M.; Mortimer, M. More Rice, Less Water—Integrated Approaches for Increasing Water Productivity in Irrigated Rice-Based Systems in Asia. *Plant Prod. Sci.* **2005**, *8*, 231–241. [CrossRef]
25. Allen, R.G.; Walter, I.A.; Elliott, R.L.; Howell, T.A.; Itenfisu, D.; Jensen, M.E.; Snyder, R.L. (Eds.) *Technical Committee on Standardization of Reference Evapotranspiration*; American Society of Civil Engineers: Reston, VA, USA, 2005.